Silicon (2022) 14:4183–4196
https://doi.org/10.1007/s12633-021-01202-4

ORIGINAL PAPER

Dry Machining Performance Studies on TiAlSiN Coated Inserts in Turning of AISI 420 Martensitic Stainless Steel and Multi-Criteria Decision Making Using Taguchi - DEAR Approach

C. Moganapriya[1] · R. Rajasekar[1] · T. Mohanraj[2] · V. K. Gobinath[3] · P. Sathish Kumar[4] · C. Poongodi[5]

Received: 14 November 2020 / Accepted: 11 June 2021 / Published online: 20 June 2021

Abstract
The key objective of this research study is to examine the performance of TiAlSiN coated insert while performing dry machining of AISI 420 martensitic stainless steel on quantified output responses. This paper seeks to optimize process parameters namely speed, feed, and depth of cut during turning process, such as surface roughness, flank wear, and material removal rate simultaneously. TiAlSiN thin film was coated on the carbide tool through high power impulses magnetron sputtering. To confirm the existence of coated elements, SEM and XRD studies were performed. For coated and pure inserts, microhardness was measured, whereas the TiAlSiN coated tool possesses 43.34% higher than pure inserts. The dry machining was performed with three process parameters, each in three phases. The experimentation was performed based on Taguchi's design of experiments (DoE). In this study, a Multi-Criteria decision making (MCDM) approach encompassing Data Envelopment Analysis based Ranking Methodology (DEAR) with Taguchi's design was applied. The multi-response performance index (MRPI) was calculated and their impact on the machining parameters was scientifically examined. The parameter combination of cutting speed: 240 m/min; feed rate: 0.20 mm/rev and depth of cut: 0.50 mm was observed to be the optimal input parameters.

Keywords AISI 420 steel · MRR · Surface roughness · Flank wear · DEAR · Multi-criteria decision making

1 Introduction

The best candidate for minimizing health and environmental risks is machining without coolant or dry machining. Thus dry machining has brought considerable attention to the development of safe and clean environments among researchers and processing industries, as it eliminates the cutting fluid entirely. A variety of benefits can be obtained by dry manufacturing, including no emissions to the atmosphere, water and earth; no work hazards; and considerable cost savings, as there is zero fluid maintenance and disposal costs. However, high heat generation and increased friction in dry cutting contributes to high wear of cutting tool and builtup edge impacting the machined surface finish. Therefore, efficient dry cutting includes steps to counterbalance the positive effects of lubricants, such as optimal process parameter, application of coatings, change in tool geometry and the tool material [1]. Owing to better resistance in corrosion, AISI 420 stainless steel is majorly utilized in aircraft, medical, and food storage industries. In addition to basic elements like iron, carbon, nickel, it also contains 13 to 30% of chromium approximately [2]. Due to their high ductility, poor thermal conductivity, superior hardness factor, and larger friction coefficient, these steels have major complications in cutting processes.

The characteristics of cut material have major impact on the performance of machining process, which is typically referred to as "machinability". However, the surface feature is an

✉ R. Rajasekar
rajasekar.cr@gmail.com

[1] Department of Mechanical Engineering, Kongu Engineering College, Perundurai, Tamilnadu, India

[2] Department of Mechanical Engineering, Amrita School of Engineering, Amrita Vishwa Vidyapeetham, Coimbatore, India

[3] Department of Mechatronics Engineering, Kongu Engineering College, Perundurai, Tamilnadu, India

[4] Department of Mining Engineering, Indian Institute of Technology, Kharagpur, West Bengal, India

[5] Department of Information Technology, Vivekanandha College of Engineering for Women, Elaiyampalayam, Tamilnadu, India

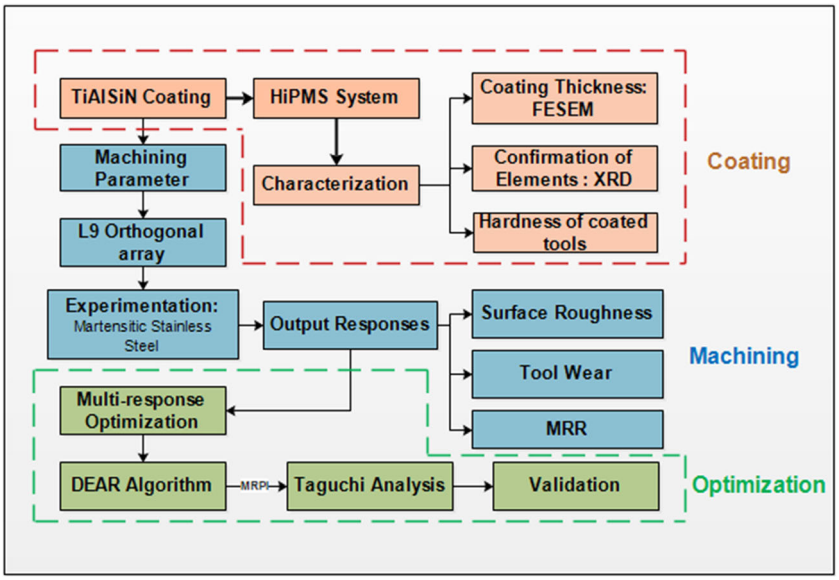

Fig. 1 Methodology of research work

essential criterion for assessing the efficiency of machine tools and machined parts. Therefore, it is extremely necessary to study the mechanical performance of machined components to obtain the required surface quality [3].

Recently, many optimization models for surface roughness were considered with processing factors, which helps to simulate and optimize the cutting process [4]. The examination of surface roughness has been determined by various researchers during dry machining operation of steel. El-Tamimi analyzed AISI 420 stainless steel at numerous machining criteria by adopting carbide cutting tools. The major prominent influences were determined through mean effect and interaction plots [5]. The efficiency of wiper coated insert on hard turning of AISI 420 steel was examined through tool wear and surface quality analysis [6].

However, TiAlN, AlTiN, TiN hard coatings have been utilized widely for cutting due to extensive mechanical properties [7–9], Generally, incorporation of Si onto TiAlN improves thermal stability, tribological behavior and high-temperature oxidation resistance of the coatings [10, 11]. These sorts of microstructure refine its grains and enhance the coating hardness. The advanced features of TiAlSiN confirm the cutting needs of Inconel 718 through severe work-hardening and high cutting temperature [12].

The high-power impulse magnetron sputtering (HiPIMS) attracts several researchers due to its higher level of ionization rate

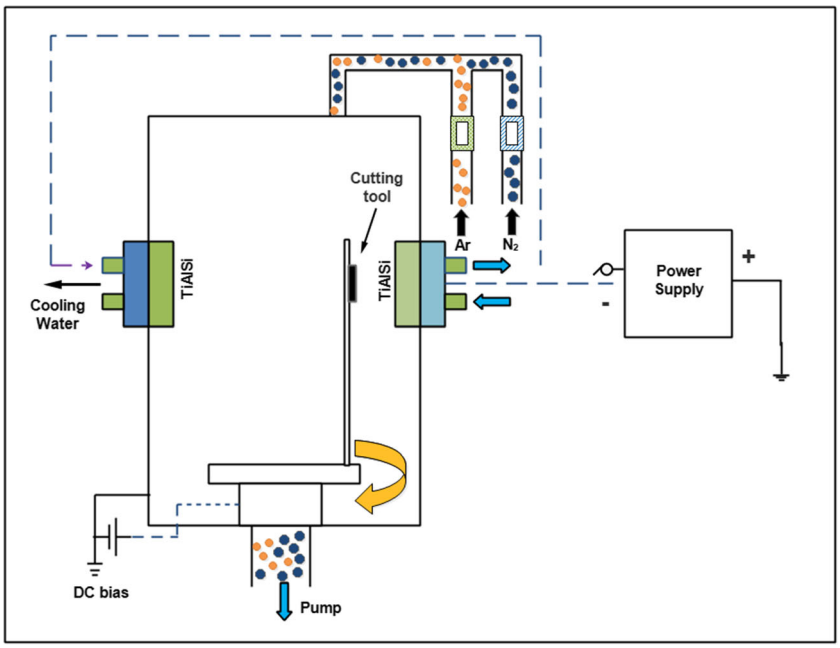

Fig. 2 HiPIMS coating system

Table 1 Deposition parameter

S. No.	Operating parameter	Value
1	Base pressure	2 X 10 $^{-3}$ Pa
2	Pulse width	200 μs
3	Frequency	50 Hz
4	Bias voltage	400 V
5	Supply voltage	950 V
6	Pressure	0.8 Pa

of the target material [13]. This specific feature helps to monitor the deposition process directly and deposit hard coatings with improved density, enhanced crystallinity, and better adhesion [14]. Moreover, HiPIMS-coating achieved homogeneity in thickness even on complex tools, since the altered bias voltage deposits large number of ions throughout the entire substrate surfaces and obtain weak shadowing effect [15, 16]. Therefore, this technology has tremendous prospective in the area of cutting tool inserts. In general, machining process involves, multiple performance measurement like tool wear, surface roughness, material removal rate etc. These multiple responses majorly influence the selection of process parameters. Hence, the conventional method employed for optimizing single response seems to be in appropriate for machining process, which measures more than one responses. To overcome this problem and to achieve machining effectiveness, multi-response optimization is required [17–19]. Therefore, multi-response optimization algorithms such as weight assignment method, Grey relational analysis (GRA), Technique for Order of Preference by Similarity to Ideal Solution (TOPSIS), Taguchi- Data Envelopment Analysis based Ranking Methodology (DEAR) analysis have been used for optimizing the process parameters [20–24]. RSM approach is used for development of predictive modeling and the data representation in the RSM technique is more tedious, which requires more experiments [25].

However, weight assignment is very easy; the accuracy of the forecast is not desirable. A complex approach is to identify the grey distinct coefficient based on the existence of the process constraint [26]. The artificial neural network (ANN) based method, enhances the forecast accuracy. The numerical complexity requires several steps for achieving the enhanced prediction accuracy [27]. Machining performance can be predicted through ANN, fuzzy logic, and machine learning algorithms [28]. The Taguchi-DEAR approach effectively estimates the optimum combination of process parameters [29, 30].

Table 2 Composition of the workpiece

Composition	C	Si	Mn	Cr	Ni	Mo	P	S
(wt.%)	0.32	0.55	0.46	12.3	0.15	0.00	0.026	0.024

Table 3 Machining parameters

Factors	Unit	Levels		
		1	2	3
Cutting speed (A)	m/min	120	180	240
Feed rate (B)	mm/rev	0.1	0.15	0.2
Depth of cut (C)	mm	0.1	0.25	0.5

Though several optimization techniques are applied to optimize production process parameters, there still persist a high level of expectation for identifying a simpler and efficient multi-criteria decision making technique (MCDM). In connection to the same, Taguchi – Data Envelopment Analysis Ranking (DEAR) technique has proven to be efficient in terms of simplest methodology and similar results in line with the output values obtained from other optimization tools [29–31]. Several authors employed this technique to optimize multiple responses during machining [29–31]. Since, the adoption of Taguchi- DEAR technique for optimizing the machining process parameters of AISI 420 steel is unexplored, this research work filled the research gap by analysing the same by using TiAlSiN coated WC insert.

AISI 420 stainless steel is majorly utilized in aircraft, medical and food storage industries. The referred material is typically machined using WC tools. In addition, it is evident from the research reports that the following coating materials namely TiAlN, AlTiN, TiN has proven substantial machining performance. TiAlSiN coating is developed by incorporation of Si onto TiAlN. The former offers substantial increment in thermal stability, tribological properties and high-temperature oxidation resistance. The utilization of TiAlSiN coated inserts for machining AISI 420 steel is unexplored. Hence, the suitability of TiAlSiN coated inserts in machining AISI 420 steel is experimentally investigated in this research work. Moreover, the research study also extended in employing a simplified optimizing tool namely Taguchi-

Table 4 L_9 OA design

S.No.	A	B	C
1	1	1	1
2	1	2	2
3	1	3	3
4	2	1	2
5	2	2	3
6	2	3	1
7	3	1	3
8	3	2	1
9	3	3	2

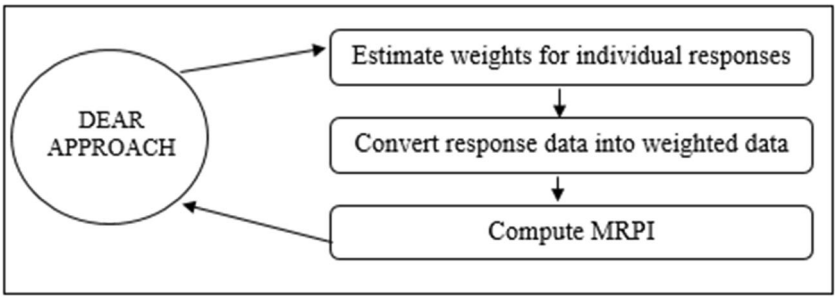

Fig. 3 DEAR approach

DEAR technique for achieving appropriate machining process parameters in an efficient manner.

The aim of this research work is to employ Taguchi-DEAR analysis inorder to create an optimization model for multiple responses while machining AISI 420 martensitic stainless steel. The primary goal of this paper is to assist users of AISI 420 steel in obtaining the best process conditions for their application. The following objectives were defined in this research work to meet the targets:

1. To develop Titanium Aluminum Silicon Nitride (TiAlSiN) hard coating material on tool insert.
2. To identify optimal cutting conditions for dry turning of AISI 420 steel by adopting Taguchi-DEAR analysis (cutting speed, cutting depth and feed speed).

2 Experimental Details

The overall work plan of this research work is depicted in Fig. 1. Initially, the cutting tool insert was coated with TiAlSiN thin flim using commercially available HiPIMS apparatus. The layer thickness of coated insert was measured through Field Emission Scanning Microscope (FESEM) and elemental analysis was determined through X-Ray Diffraction Analysis (XRD). Hardness of coated and uncoated insert was measured. Machining experiments were conducted based on designed Taguchi's L_9 orthogonal array (OA) with three input and three output parametes. The output responses like SR, TW, and MRR were measured for each experiment. After finding all the responses, MCDM was performed by adopting Taguchi-DEAR analysis. The results of optimization has been validated through confirmation experiment.

2.1 Coating Deposition

The thin film TiAlSiN coating was accomplished on the surface of uncoated tungsten carbide turning tool inserts through commercially available HiPIMS apparatus as depicted in Fig. 2 [12]. The operating conditions were listed in Table 1. To achieve high degree of cleanliness, all the uncoated inserts were mechanically polished and cleaned ultrasonically before deposition. Again, the substrates (tools) were cleaned for 30 min through glow discharge operating at 1000 V substrate bias voltage and 1.5 Pa argon pressure.

The mixture of high purity argon and nitrogen gases (99.99%) was used and the temperature was sustained at 150^{o} C throughout the deposition process. The deposition chamber was equipped with 99.99% purified TiAlSiN (Ti:

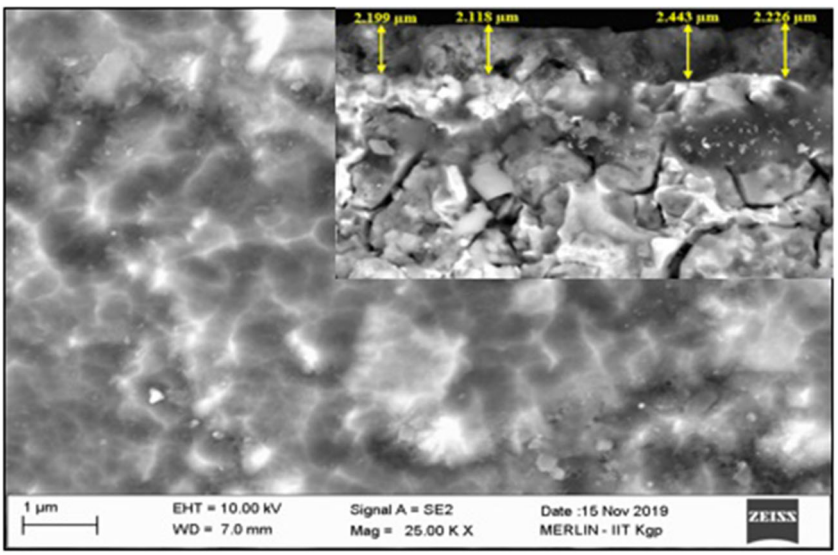

Fig. 4 Cross-sectional FESEM morphology

0.64, Al: 0.3, Si: 0.06) substrates, which are in rectangular shapes and mounted on the inner walls of the deposition chamber. To enhance the adhesion between coating and substrate, nitrogen ion implantation was utilized before the deposition of TiAlSiN thin film. The substrate holder was subjected to continuous rotation between sputtering targets through stepper motor. Thin-film TiAlSiN layer was sputter-coated by maintaining the process parameter mentioned in Table 1 [12].

2.2 Characterization of the Coated Insert

TiAlSiN thin film coatings were characterized through series of systematic techniques. Cross-sectional coating thickness was characterized using FESEM (make: Carl Zeiss EVO60). The existence of coating materials has been confirmed using XRD analysis (make: 'X' Pert Pro, Panalytical, Netherlands). Vickers microhardness tester was employed to measure the microhardness of the tools before and after the coating. An average of four measurements was reported.

2.3 Workpiece and Process Parameters

Martensitic AISI 420 stainless steel has been used as the workpiece material for this research study. The elemental composition of AISI 420 martensitic stainless steel is depicted in Table 2.

From the previous studies, significant process parameters such as cutting speed, feed rate, and depth of cut were selected for machining AISI 420 martensitic stainless steel as listed in Table 3. Workpiece with 40 mm diameter and 95 mm length was used for dry turning experimentation.

2.4 Selection of Output Measures

The quality of machining can be determined by machining features such as tool wear (TW), surface roughness (SR), and material removal rate (MRR). Hence, these parameters have been selected as the output performance measures in this present work. Tool wear has been computed using profile projector. The average of three values was reported to evade the experimental errors. The average centre line surface roughness for the machined workpiece has been measured through the Mitutoyo surface roughness tester with a measuring speed of 0.5 mm/s. The difference in weight of workpiece before and after machining was employed to calculate MRR in g/min.

2.5 Orthogonal Array

The present work considers three input parameters such as cutting speed, feed rate, and depth of cut, and hence, L_9 OA was employed by adopting the Taguchi DoE as listed in Table 4, which depicts the choice of parameters at different levels.

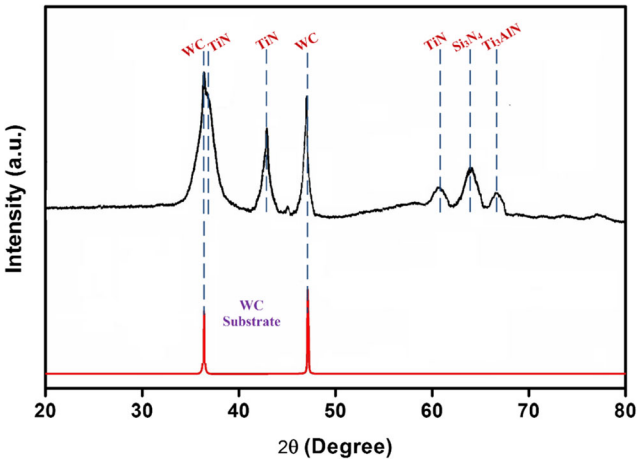

Fig. 5 XRD analysis of TiAlSiN coated tool

2.6 DEAR: Data Envelopment Analysis Based Ranking Methodology

In the DEAR analysis, measured initial responses are assigned to a ratio called MRPI, which is employed to determine the optimal set of parameters [30]. The systematic procedure for the DEAR approach is depicted in Fig. 3.

1. Estimate weight for individual responses: The response weight is the ratio of responses at any run to the summation of the responses of all tests performed [29]. Weights are computed through the equations as described below

$$W_{Tw} = \frac{1/Tw}{\sum 1/Tw} \text{ Smaller the better} \quad (1)$$

$$W_{SR} = \frac{1/SR}{\sum 1/SR} \text{ Smaller the better} \quad (2)$$

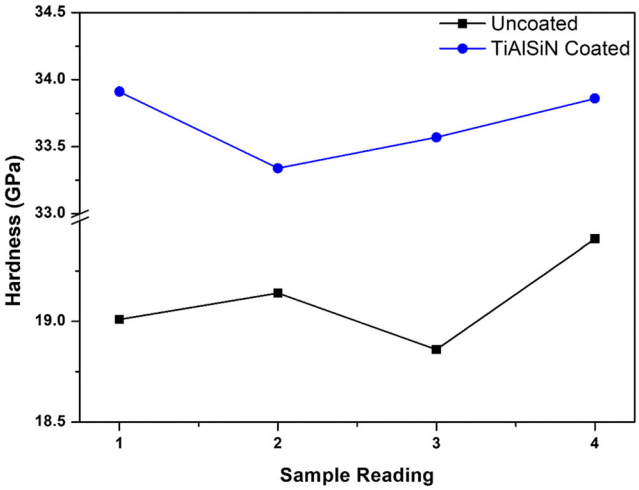

Fig. 6 Hardness of coated and uncoated tool

Table 5 Experimental data

Run order	Cutting speed	Feed	Depth of cut	SR μm	MRR g/min	TW mm
1	120 (A1)	0.10 (B1)	0.10 (C1)	0.528	0.2275	0.0170
2	120 (A1)	0.15 (B2)	0.25 (C2)	0.708	0.6550	0.0230
3	120 (A1)	0.20 (B3)	0.50 (C3)	1.317	1.3175	0.0110
4	180 (A2)	0.10 (B1)	0.25 (C2)	0.339	0.6600	0.0120
5	180 (A2)	0.15 (B2)	0.50 (C3)	0.457	1.0275	0.0160
6	180 (A2)	0.20 (B3)	0.10 (C1)	0.511	0.5625	0.0100
7	240 (A3)	0.10 (B1)	0.50 (C3)	0.505	1.4975	0.0130
8	240 (A3)	0.15 (B2)	0.10 (C1)	0.319	0.5225	0.0160
9	240 (A3)	0.20 (B3)	0.25 (C2)	0.587	1.3150	0.0180

$$W_{MRR} = \frac{MRR}{\sum MRR} \text{ Larger the better} \quad (3)$$

The tool wear and surface roughness have been minimized and MRR has been maximized for optimization. Hence, the reciprocal of tool wear and surface roughness was considered for weight calculation [29].

2. Compute the product of each response and its weight for generating weighted data from the below equations

$$T = W_{Tw} * Tw \quad (4)$$

$$S = W_{SR} * SR \quad (5)$$

$$M = W_{MRR} * MRR \quad (6)$$

3. Determine the ratio of 'higher the best response' (MRR) to the summation of all 'lower the best responses' (SR and TW), which denotes MRPI

$$MRPI = \frac{M}{(T+S)} \quad (7)$$

2.7 Taguchi Analysis

By adopting DEAR analysis, multiple responses have been converted into single response called MRPI. The computed MRPI values were reflected as the single response and optimized using Taguchi's DoE. A higher signal-to-noise ratio (S/N) for MRPI is preferred for the best optimal solution and hence, the larger the better criteria is selected to calculate the S/N.

$$\frac{S}{N}\text{ratio} = -10\log\sum\left(1/y^2\right)/n \quad (8)$$

The highest S/N represents the best optimal solution for every input parameter [32].

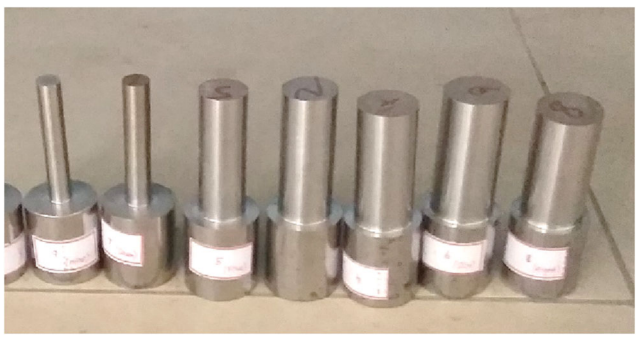

Fig. 7 Machined samples

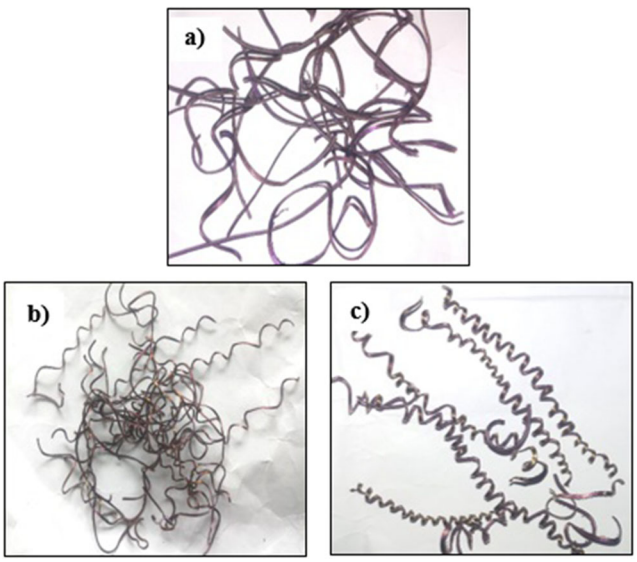

Fig. 8 Chip morphology: **a** experiment 2; **b** experiment 5; **c** experiment 9

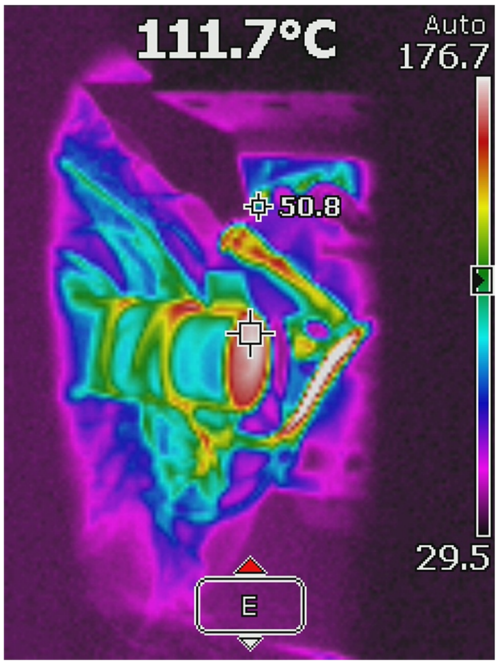

Fig. 9 Thermal image for experiment 9

3 Results and Discussion

3.1 Microstructure of Coated Tool

The surface morphology and cross-sectional SEM image confirms the presence of TiAlSiN coating as depicted in Fig. 4. TiAlSiN layer structure could be identified clearly, which confirms the nano-composite structure (nc-Ti_3AlN/a-Si_3N_4) as observed by few researchers [12]. The average cross-sectional thickness of the coated layer was found to be 2.246 μm.

Table 6 Response table for S/N ratio of SR

Level	Cutting speed	Feed rate	Depth of cut
1	2.052	6.959	7.101
2	7.343	6.575	5.674
3	6.829	2.689	3.448
Delta	5.291	4.270	3.653
Rank	1	2	3

3.2 Elemental Analysis

Figure 5 demonstrates the XRD pattern of deposited TiAlSiN coating and uncoated WC insert. According to Fig. 5, WC (JCPDF No.: 89–2727), Ti_3AlN (JCPDF No.: 37–1140), Si_3N_4 (JCPDF No.: 51–1334), and TiN (JCPDF No.: 87–0631) from ICCD card are matching with these preference orientations. It was also observed that no AlN segments existed in the XRD pattern because of high Ti-Al ratios, which suggested that the Al element probably exists as a compound of Ti_3AlN with a crystal structure similar to NaCl [33]. Figure 5 describes (111), (200), (220) of TiN and Ti_3AlN planes [12].

3.3 Hardness of the Coated Tool

The average hardness of the TiAlSiN coated tool was measured as 33.7 GPa, whereas the uncoated tool possesses 19.1 GPa and the same has been portrayed in Fig. 6. The microhardness of the coated tool was 43.34% higher than uncoated tool. TiAlSiN coatings possess enhanced mechanical properties than uncoated tools owing to the addition of Si, which constitutes the crystalline phase of nanocomposite

Fig. 10 S/N ratio plot for SR

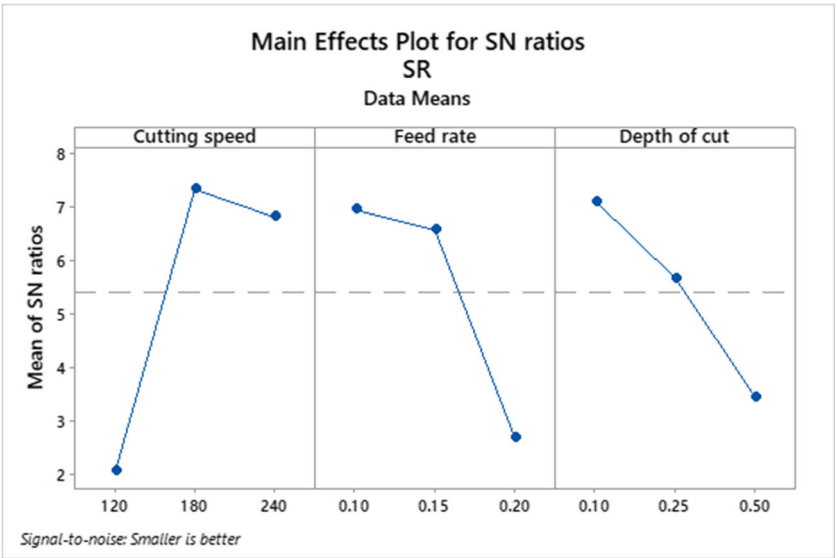

Table 7 Analysis of variance for SR

Source	DF	Adj SS	Adj MS	F-Value	*p* value	% Contribution
Cutting speed	2	0.31861	0.15931	11.54	0.008	46.43
Feed rate	2	0.21857	0.10929	7.92	0.032	31.87
Depth of cut	2	0.14894	0.07447	5.39	0.046	21.69
Error	2	0.02761	0.01381			
Total	8	0.71373				

Table 8 Response table for S/N ratio of TW

Level	Cutting speed	Feed rate	Depth of cut
1	35.78	37.18	37.10
2	38.11	34.87	35.36
3	36.18	38.02	37.60
Delta	2.34	3.16	2.24
Rank	2	1	3

Ti_3AlN. It was draped in the amorphous phase of a-Si_3N_4 at the nanometer level [10, 11]. This form of crystal structure can refine TiAlN grains and strengthen the hardness of coatings owing to the effect of hall patch [34, 35].

3.4 Dry Machining of AISI 420 Martensitic Stainless Steel

The dry turning operations have been performed based on L_9 OA on AISI 420 martensitic stainless steel. Table 5 depicts the experimental findings for all 9 experiments. Figure 7 shows the images of machined samples.

The morphology of collected chips from machining are presented in Fig. 8. The study of chip characteristics exhibits the transformation of chip color from golden to blue burnt through the entire duration of machining. It is disclosed that the rise in machining temperature was higher, which was distinctly observed from the experiments with higher tool wear as portrayed in Fig. 8a, c. The thermal image for experiment 9 captured through infrared thermal imager is depicted in Fig. 9. The color of the chips transformed into blue burnt owing to the increase in cutting temperature. This phenomenon leads to excessive tool wear. Golden color helical chip was produced till the machining duration of 3 min. Color of the chip hastily varied to blue and burnt blue while machining for 10 min as shown in Fig. 8c. The burnt blue color represents the inordinate temperature generated in machining (50.8 °C) as depicted in Fig. 9. It led to rapid deterioration of cutting edge and sharpness of tool [36].

3.5 Single Response Optimization of Individual Responses

The individual responses such as SR, MRR, and TW were analyzed separately through the Taguchi's S/N. For SR and TW 'smaller the better' and for MRR 'larger the better' characteristics was applied to calculate the S/N ratio.

3.5.1 Effect of Process Parameter on Surface Roughness

As depicted in Fig. 10, cutting speed: 180 m/min; feed rate: 0.10 mm/rev and depth of cut: 0.10 mm were found to be the best optimal parameter for SR. However, in order to predict optimum values of performance characteristics, substantial contributions of process parameters must be known.

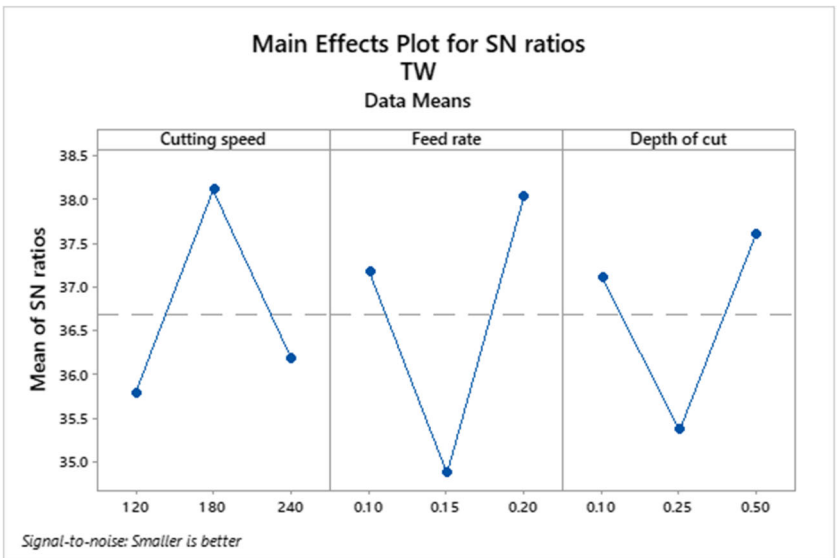

Fig. 11 S/N ratio plot for TW

Table 9 Analysis of variance for TW

Source	DF	Adj SS	Adj MS	F-Value	*p* value	% Contribution
Cutting speed	2	0.000034	0.000017	1.28	0.045	28.76
Feed rate	2	0.000056	0.000028	1.99	0.034	44.71
Depth of cut	2	0.000030	0.000015	1.18	0.044	26.51
Error	2	0.000013	0.000002			
Total	8	0.000133				

The response table depicts the mean of S/N ratio for SR at a particular level of a process parameter as listed in Table 6. Cutting speed (Delta 5.291, Rank = 1) has the largest effect on S/N ratio, followed by feed rate (Delta 4.270, Rank = 2), and depth of cut (Delta 3.653, Rank = 3).

From the results of ANOVA table, cutting speed has the highest contribution (46.43%), whereas feed rate and depth of cut showed 31.87% and 21.69% on surface roughness as depicted in Table 7. Reduction in the feed rate and depth of cut sharply reduced the surface roughness. The output response was predicted at the optimal parameter setting (cutting speed: 180 m/min; feed rate: 0.10 mm/rev and depth of cut: 0.10 mm) as 0.2694 μm. The experiment has been conducted at optimized setting and SR was found to be 0.2913 μm.

3.5.2 Effect of Process Parameter on Tool Wear

From Fig. 11, the best optimal parameter for TW was determined as cutting speed: 180 m/min; feed rate: 0.20 mm/rev and depth of cut: 0.50 mm.

The response table provides the mean of S/N ratio for TW. Feed rate significantly affects tool wear followed by cutting speed and depth of cut as listed in Table 8.

From Table 9, it was found that feed rate was the highest contributor to tool wear (44.71%) because it increases the cutting temperature at cutting edge of a tool. The higher temperature gradient in the cutting zone causes tool to lose its strength [36]. Followed by feed rate, cutting speed and depth of cut affects tool wear by 28.76% and 26.51%. The output response was predicted at optimized setting (cutting speed: 180 m/min; feed rate: 0.20 mm/rev; depth of cut: 0.50 mm) and it was estamiated as 0.0952 mm. The experiment was conducted at optimized setting and TW was found to be 0.1013 mm.

3.5.3 Effect of Process Parameter on MRR

The best optimal parameter for MRR was portrayed in Fig. 12. It was evaluated as cutting speed: 240 m/min; feed rate: 0.20 mm/rev and depth of cut: 0.50 mm. From the response table for S/ N ratio of MRR, depth of cut contributes majorly to MRR followed by cutting speed and feed rate as portayed in Table 10. These findings are in agreement with previous work [37].

From Table 11, it was found that depth of cut significantly affects MRR by 69.89%. Increase in depth of cut

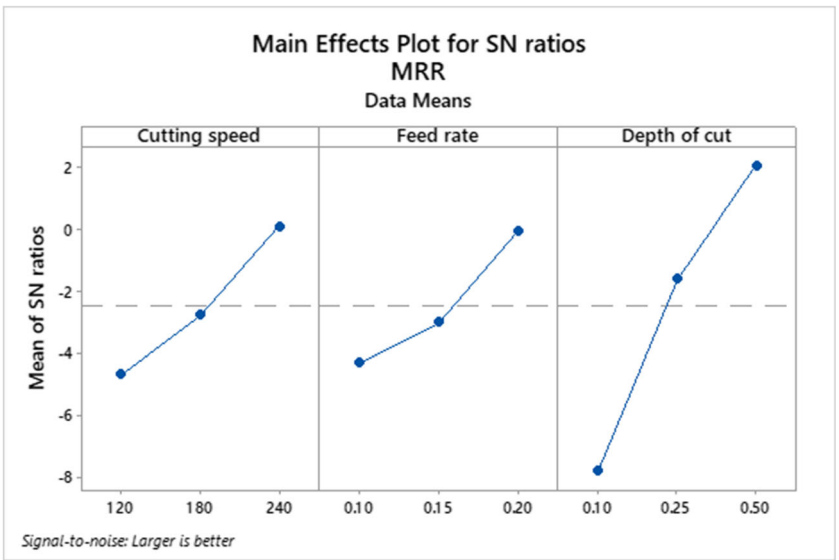

Fig. 12 S/N ratio plot for MRR

Table 10 Response table for S/ N ratio of MRR

Level	Cutting speed	Feed rate	Depth of cut
1	−4.71351	−4.32072	−7.83207
2	−2.79034	−3.02594	−1.63526
3	0.08253	−0.07467	2.04600
Delta	4.79604	4.24604	9.87806
Rank	2	3	1

predominantly increases MRR. Cutting speed and feed rate nominally affects MRR by 17.95% and 12.14%. The output response was predicted as 1.572 g/min mm at optimized setting (cutting speed: 240 m/min; feed rate: 0.20 mm/rev and depth of cut: 0.50 mm). The experiment was conducted at optimized setting and MRR was found to be 1.528 g/min.

3.6 Multi-Criteria Decision Making for Turning Process Using Taguchi-DEAR Analysis

To examine the combined influence of each input parameter on multiple outputs and to determine the optimal process parameters for three responses, MRPI has been calculated through DEAR approach. The MRPI of each experiment was computed using Taguchi-DEAR technique for varying configurations of input variables. Table 12 presents the associated MRPI for input parameters at all stages. For the respective level of each process variable, the parameters were determined by combining all the MRPI levels. The maximal level of any process parameter represents the optimum input level, which in turn determines the output measures in any process. Table 12 indicates the optimum combination of input parameters for dry turning operation as follows: Speed: 240 m/min; feed: 0.20 mm/rev; cutting depth: 0.50 mm, respectively.

The fluctuation of the response curve towards the horizontal axis shows the significance of machinability of AISI 420 martensitic stainless steel by TiAlSiN coated insert. It was found that cutting depth had a greater effect on the measurement of output performance. As depicted in Fig. 13, Speed: 240 m/min; feed: 0.20 mm/rev; depth of cut: 0.50 mm were observed to be the best optimal parameter for MRPI.

Analysis of variance (ANOVA) was performed to examine the influence of cutting parameters on the responses. The

Table 11 Analysis of variance for MRR

Source	DF	Adj SS	Adj MS	F-Value	*p* value	% contribution
Cutting speed	2	0.27422	0.137108	34.21	0.028	17.95
Feed rate	2	0.18540	0.092700	23.13	0.041	12.14
Depth of cut	2	1.06743	0.533715	133.15	0.007	69.89
Error	2	0.00802	0.004008			
Total	8	1.53507				

Table 12 Calculation of MRPI

Exp. no.	Weights			MRPI
	SR	MRR	TW	
1	0.105340	0.029223	0.092778	0.11623
2	0.078559	0.084136	0.068575	0.96350
3	0.042232	0.169236	0.143385	3.89825
4	0.164070	0.084778	0.131436	0.97826
5	0.121706	0.131985	0.098577	2.37100
6	0.108845	0.072254	0.157723	0.71058
7	0.110138	0.192357	0.121325	5.03619
8	0.174357	0.067116	0.098577	0.61311
9	0.094753	0.168915	0.087624	3.88347

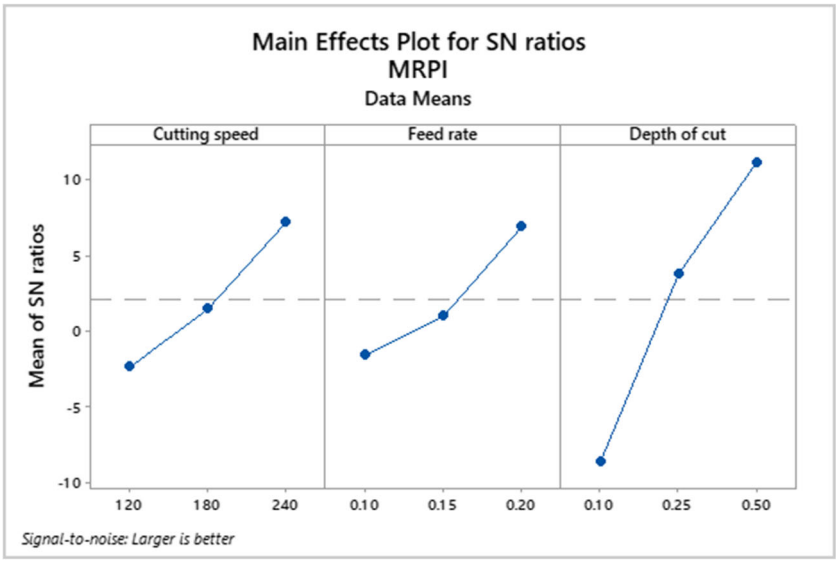

Fig. 13 S/N ratio plot for MRPI

percentage contribution (PC) of each parameter on the responses is calculated from analysis of variance as depicted in Table 13. The depth of the cutting is 63.32% the most prominent, followed by cutting speed which influences 22.26% and feed rate contributes by 13.39%. Furthermore, all the three parameters (cutting speed, depth of cut and feed rate) had statistical significance of 95% of the S / N ratios as respective F-calculated values are higher than their F0.05-tabulated standards. The *p* value for all the parameters is less than 0.05, which indicates the physical significance of the parameter. The regression for predicting MRPI is given in Eq. 9. It was observed that the predicted MRPI was maximum as compared to an average of all MRPI values found through experimental data.

Table 13 Analysis of variance for MRPI

Source	DF	Adj SS	Adj MS	F-Value	p Value	PC
Cutting speed	2	5.7269	2.8634	21.64	0.032	22.26
Feed rate	2	3.4441	1.7221	13.02	0.048	13.39
Depth of cut	2	16.2880	8.1440	61.55	0.016	63.32
Error	2	0.2646	0.1323			
Total	8	25.7236				

DF Degree of freedom
Adj. SS Adjusted sums of squares
Adj. MS Adjusted mean squares
PC Percentage contribution

Table 14 Confirmation experiment

S.No.	Process parameter		Measured output	
	Parameter	Value	Parameter	Value
1	Cutting speed	240 m/min	Surface Roughness	0.347 μm
2	Feedrate	0.2 mm/rev	Tool Wear	0.0117 mm
3	Depth of cut	0.5 mm	MRR	1.263 g/min
	Predicted MRPI 4.975		MRPI for Confirmation Experiment 4.9153	

Fig. 14 Cutting chip at optimized setting

$$\mathbf{MRPI} = -\mathbf{3.70} + \mathbf{0.01265}\ \text{Cutting speed} + \mathbf{7.87}\ \text{Feed rate} + \mathbf{8.13}\ \text{Depth of cut} \quad (9)$$

3.7 Confirmation Experiment

The validation study intends to confirm the optimal combination of process parameters derived from the methodology. A validation experiment was performed in the present study employing the optimum levels of key factors. The output responses from the validation experiment were detected as SR: 0.347 μm; TW: 0.0117 mm; MRR: 1.263 g/min at the optimal process parameter setting as listed in Table 14. MRPI for the confirmation experiment was determined as 4.9153, which was 1.2% distinct from the predicted MRPI value. Hence, in the current analysis, the optimum combination of process parameters was validated satisfactorily with 98.8% prediction accuracy.

The chips produced during the confirmation experiment are depicted in Fig. 14. It was revealed that machining at optimal parameters results in the formation of golden and lighter color chips, which was owing to lower cutting temperature (26.2 °C) as portrayed in Fig. 15. It results in reduction of tool wear.

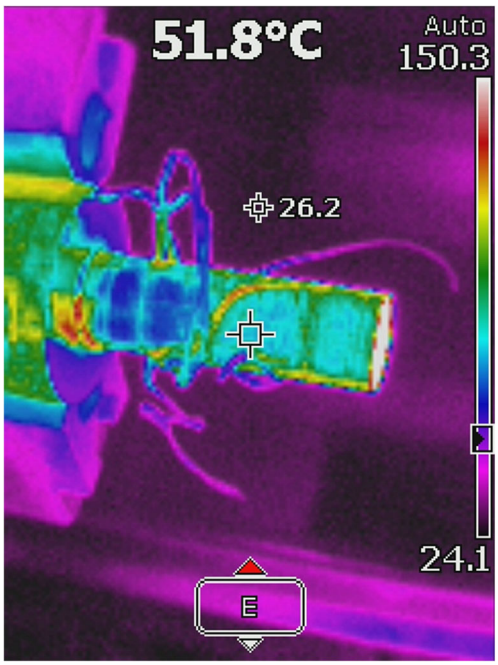

Fig. 15 Thermal image of confirmation experiment

4 Conclusions

The machining performance of AISI 420 martensitic stainless steel with TiAlSiN hard coating was studied. The coating was deposited effectively on the CNC turning insert through the HiPIMS process. Coating thickness was estimated as 2.246 μm. The coating elements like Ti, Al, Si, W, and C have been confirmed by an XRD examination. The microhardness of the TiAlSiN coated inserts exhibit high hardnesses of 33.7 GPa, which is 43.34% higher than the uncoated insert, and it significantly reduces tool wear. DEAR has been used as multi-criteria decision making technique to optimize the parameters for multiple responses. The results showed that cutting speed of 240 m/min, the feedrate of 0.20 mm/rev, and depth of cut of 0.50 mm were found as an optimal parameter that minimizes TW, SR, and maximizese MRR. The results from ANOVA showed that the depth of cut had major contribution of 63.32% on MRPI followed by speed and feed of 22.26% and 13.39% respectively. The responses measured from verification test were found to be surface roughness: 0.347 μm, flank wear: 0.0117 mm, and MRR: 1.263 g/min. The relationship between predicted and experimental values was solid. With 98.8% predicted accuracy, the proposed Taguchi-DEAR model can predict output response accurately.

Nomenclature ANOVA, Analysis of variance; ANN, Artificial neural network; DoE, Design of Experiemnts; DEAR, Data Envelopment Analysis based Ranking Methodology; FESEM, Field Emission Scanning Electron Microscope; GRA, Grey relational analysis; HiPIMS, High power impulse magnetron sputtering; MRPI, Multi-response performance index; MRR, Material removal rate; RSM, Response surface methodology; S/N, Signal-to-noise ratio; SEM, Scanning electron microscope; SR, Surface roughness; TOPSIS, Technique for Order of Preference by Similarity to Ideal Solution; TW, Tool wear; XRD, X-ray Diffraction Analysis

Acknowledgments No funds, grants, or other support was received

Code Availability Not applicable.

Author Contributions All authors discussed the content of the article based on their domain expertise on the subjects presented. C. Moganapriya performed the experiments and analyzed the data through statistical approach. P. Sathish Kumar characterized the coatings through SEM and XRD. T. Mohanraj optimized the results through DEAR approach. V. K. Gobinath and C. Poongodi executed the confirmation experiment. C. Moganapriya drafted the paper and revised the manuscript. R. Rajasekar supervised the study and discussed the results, proofread the manuscript and confirmed its findings. All authors read and approved the final manuscript.

Data Availability Included in the manuscript.

Declarations

Conflict of Interests The author(s) declared no potential conflicts of interest concerning the research, authorship, and/or publication of this article.

Consent to Participate Not applicable.

Consent for Publication Not applicable.

References

1. Sharma N, Gupta K (2019) Influence of coated and uncoated carbide tools on tool wear and surface quality during dry machining of stainless steel 304. Mater Res Exp 6(8):086585
2. El-Tamimi AM, Soliman MS, El-Hossainy TM, Muzher JA (2010) Developed models for understanding and predicting the machinability of a hardened martensitic stainless steel. Mater Manuf Process 25(8):758–768. https://doi.org/10.1080/10426910903447337
3. Benardos P, Vosniakos G-C (2003) Predicting surface roughness in machining: a review. Int J Mach Tools Manuf 43(8):833–844
4. Asiltürk I, Neşeli S (2012) Multi response optimisation of CNC turning parameters via Taguchi method-based response surface analysis. Measurement 45(4):785–794
5. El-Tamimi A, El-Hossainy T (2008) Investigating the machinability of AISI 420 stainless steel using factorial design. Mater Manuf Process 23(4):419–426
6. Noordin M, Venkatesh V, Sharif S (2007) Dry turning of tempered martensitic stainless tool steel using coated cermet and coated carbide tools. J Mater Process Technol 185(1–3):83–90
7. Ucun İ, Aslantaş K, Gökçe B, Bedir F (2014) Effect of tool coating materials on surface roughness in micromachining of Inconel 718 super alloy. Proc Inst Mech Eng B J Eng Manuf 228(12):1550–1562
8. Akhtar W, Sun J, Chen W (2016) Effect of machining parameters on surface integrity in high speed milling of super alloy GH4169/Inconel 718. Mater Manuf Process 31(5):620–627
9. Ibrahim GA, Che Haron CH, Ghani JA, Yazid A, Zaid M (2011) Performance of PVD-coated carbide tools when turning Inconel 718 in dry machining. Advances in Mechanical Engineering (Hindawi Publishing Corporation) 3
10. Sui X, Li G, Qin X, Yu H, Zhou X, Wang K, Wang Q (2016) Relationship of microstructure, mechanical properties and titanium cutting performance of TiAlN/TiAlSiN composite coated tool. Ceram Int 42(6):7524–7532
11. Jiang C, Zhu H, Shin K, Tang Y (2017) Influence of titanium interlayer thickness distribution on mechanical properties of Ti/TiN multilayer coatings. Thin Solid Films 632:97–105
12. Li G, Li L, Han M, Luo S, Jin J, Wang L, Gu J, Miao H (2019) The performance of TiAlSiN coated cemented carbide tools enhanced by inserting Ti interlayers. Metals 9(9):918
13. Kouznetsov V, Macak K, Schneider JM, Helmersson U, Petrov I (1999) A novel pulsed magnetron sputter technique utilizing very high target power densities. Surf Coat Technol 122(2–3):290–293
14. Anders A (2014) A review comparing cathodic arcs and high power impulse magnetron sputtering (HiPIMS). Surf Coat Technol 257:308–325
15. de Monteynard A, Schuster F, Billard A, Sanchette F (2017) Properties of chromium thin films deposited in a hollow cathode magnetron powered by pulsed DC or HiPIMS. Surf Coat Technol 330:241–248
16. Wang Z, Zhang D, Ke P, Liu X, Wang A (2015) Influence of substrate negative bias on structure and properties of TiN coatings prepared by hybrid HIPIMS method. J Mater Sci Technol 31(1):37–42
17. Vignesh V, Ilangovan S, Radhika N (2020) Statistical analysis of process parameters in drilling of SS410 stainless steel. Materials Today: Proceedings
18. Garg A, Lam JSL (2016) Modeling multiple-response environmental and manufacturing characteristics of EDM process. J Clean Prod 137:1588–1601
19. Kumar H, Ilangovan S, Radhika N (2020) Optimization of cutting parameters for MRR, tool wear and surface roughness characteristics in machining ADC12 piston alloy using DOE. Tribol Ind 42(1):32–40
20. Shankar S, Mohanraj T, Pramanik A (2019) Tool condition monitoring while using vegetable based cutting fluids during milling of Inconel 625. J Adv Manuf Syst 18(04):563–581
21. Sumesh CS, Ramesh A (2018) Numerical modelling and optimization of dry orthogonal turning of Al6061 T6 alloy. Period Polytech Mech Eng 62(3):196–202. https://doi.org/10.3311/PPme.11347
22. Mohanraj T, Ragav P, Gokul E, Senthil P, Anandh K (2021) Experimental investigation of coconut oil with nanoboric acid during milling of Inconel 625 using Taguchi-Grey relational analysis. Surf Rev Lett:2150008. https://doi.org/10.1142/s0218625x21500086
23. Moganapriya C, Rajasekar R, Kumar PS, Mohanraj T, Gobinath V, Saravanakumar J (2020) Achieving machining effectiveness for AISI 1015 structural steel through coated inserts and grey-fuzzy coupled Taguchi optimization approach. Struct Multidiscip Optim:1–18
24. Muthuramalingam T, Mohan B (2014) Application of Taguchi-grey multi responses optimization on process parameters in electro erosion. Measurement 58:495–502
25. Saravanakumar D, Mohan B, Muthuramalingam T (2014) Application of response surface methodology on finding influencing parameters in servo pneumatic system. Measurement 54:40–50
26. Deepanraj B, Sivasubramanian V, Jayaraj S (2017) Multi-response optimization of process parameters in biogas production from food waste using Taguchi–Grey relational analysis. Energy Convers Manag 141:429–438
27. Jaddi NS, Abdullah S (2017) A cooperative-competitive master-slave global-best harmony search for ANN optimization and water-quality prediction. Appl Soft Comput 51:209–224
28. Gokulachandran J, Padmanaban R (2018) Prediction of remaining useful life of cutting tools: a comparative study using soft computing methods. Int J Process Manag Benchmarking 8(2):156–181
29. Manoj M, Jinu G, Muthuramalingam T (2018) Multi response optimization of AWJM process parameters on machining TiB 2 particles reinforced Al7075 composite using Taguchi-DEAR methodology. Silicon 10(5):2287–2293

30. Muthuramalingam T, Vasanth S, Vinothkumar P, Geethapriyan T, Rabik MM (2018) Multi criteria decision making of abrasive flow oriented process parameters in abrasive water jet machining using Taguchi–DEAR methodology. Silicon 10(5):2015–2021
31. Huu Phan N, Muthuramalingam T (2020) Multi criteria decision making of vibration assisted EDM process parameters on machining silicon steel using Taguchi-DEAR methodology. Silicon. 13: 1879–1885. https://doi.org/10.1007/s12633-020-00573-4
32. Moganapriya C, Rajasekar R, Ponappa K, Venkatesh R, Karthick R (2017) Influence of cutting fluid flow rate and cutting parameters on the surface roughness and flank wear of TiAlN coated tool in turning AISI 1015 steel using Taguchi method. Arch Metall Mater 62(3):1827–1832
33. Jose F, Ramaseshan R, Dash S, Jain D, Ganesan V, Chandramohan P, Srinivasan M, Tyagi A, Raj B (2011) Significance of Al on the morphological and optical properties of Ti1− xAlxN thin films. Mater Chem Phys 130(3):1033–1037
34. Chen L, Du Y, Wang AJ, Wang SQ, Zhou SZ (2009) Effect of Al content on microstructure and mechanical properties of Ti–Al–Si–N nanocomposite coatings. Int J Refract Met Hard Mater 27(4): 718–721
35. Feng C, Hu S, Jiang Y, Wu N, Li M, Xin L, Zhu S, Wang F (2014) Effects of Si content on microstructure and mechanical properties of TiAlN/Si3N4-Cu nanocomposite coatings. Appl Surf Sci 320:689–698
36. Moganapriya C, Rajasekar R, Ponappa K, Kumar PS, Pal SK, Kumar JS (2018) Effect of coating on tool inserts and cutting fluid flow rate on the machining performance of AISI 1015 steel. Mater Test 60(12):1202–1208
37. Zerti A, Yallese MA, Meddour I, Belhadi S, Haddad A, Mabrouki T (2019) Modeling and multi-objective optimization for minimizing surface roughness, cutting force, and power, and maximizing productivity for tempered stainless steel AISI 420 in turning operations. Int J Adv Manuf Technol 102(1–4):135–157